

DR. IOAN SANISLAV (Orcid ID : 0000-0003-2940-1046)

Article type : Paper

Received date: 11-Jun-2017
Revised version received date: 05-Dec-2017
Accepted date: 12-Dec-2017

Archaean crustal growth through successive partial melting events in an oceanic plateau-like setting in the Tanzania Craton

Ioan V. Sanislav^{a*}, Thomas G. Blenkinsop^b, Paul H. G. M. Dirks^a

^a Geoscience, James Cook University, Townsville, 4011, QLD, Australia; e-mail: ioan.sanislav@jcu.edu.au; phone: (+61) 07 4781 3293; fax: (+61) 07 4781 5581

^b School of Earth & Ocean Sciences, Cardiff University, Cardiff CF10 3AT, United Kingdom

Abstract

The detrital zircon population in quartzitic conglomerates from the northern Tanzania Craton yield ages between 2640 Ma and 2790 Ma which includes most of the igneous history from this part of the craton. The igneous evolution is characterised by mafic volcanism with an oceanic plateau-like geochemical signature at ~2800 Ma followed by diorite and tonalite–trondhjemite–granodiorite dominated magmatism between 2790 and 2700 Ma, which transitioned into more evolved high-K magmatism between 2700 and 2620 Ma. The ϵ_{Hf} values of the detrital zircons range from +2.4 to -1.4 and change with time from radiogenic

This article has been accepted for publication and undergone full peer review but has not been through the copyediting, typesetting, pagination and proofreading process, which may lead to differences between this version and the Version of Record. Please cite this article as doi: 10.1111/ter.12323

This article is protected by copyright. All rights reserved.

Hf pre-2700 Ma (98% positive ϵ_{Hf}) to unradiogenic Hf post-2700 Ma (41% positive ϵ_{Hf}). The petrological progression from mafic to felsic crust is reflected in the detrital age distribution and Hf isotopes and is consistent with juvenile mafic crust slowly maturing into more evolved felsic crust through a series of successive partial melting events in an oceanic-plateau-like environment.

1. INTRODUCTION

Plate tectonics is one of the fundamental processes that drive the distribution and generation of crust on the earth's surface (van Hunen and Moyen, 2012). Continental crust is largely generated above subduction zones, with secondary sites associated with rifts, hot spots and volcanic rifted margins (Stern, 2010). However, whether modern day plate tectonics was active throughout the entire Earth history is debateable (e.g. Stern, 2005; Van Kranendonk et al., 2007; Gerya, 2014), particularly for the Archaean when the rock record (e.g. lack and/or scarcity of well documented suture zones, ophiolite sequences, and UHP metamorphic rocks) makes it difficult to correlate Archaean tectonics with present-day tectonics. Field evidence such as structural juxtaposition and duplication of stratigraphy, sedimentary cycles and sedimentation histories, plutonic and volcanic age records and geophysical imaging have been used to infer or discount plate tectonic scenarios in the Archaean (e.g. Hamilton, 1998; de Wit, 1998; Jelsma and Dirks, 2002; Van Kranendonk et al., 2004; Bédard et al., 2013).

With the exceptions of an Archaean tectonic mélange in the North China Craton, interpreted to fingerprint subduction at 2500 Ma (Wang et al., 2013), and eclogites with a MORB-like geochemical signature from the Kola Peninsula, Russia (Mints et al., 2010), interpreted to indicate subduction as early as 2870 Ma, no other Archaean rocks

unequivocally indicate subduction. The general paucity of other well-documented field evidence for plate tectonics in the Archaean has been explained by the concept of intermittent and/or localised plate tectonics during the Archaean (e.g. Moyen and van Hunen, 2012; Rey et al., 2015). Since modern-day plate tectonics is dominated by spreading, subduction, and island arc accretion to continental margins, the existence of a modern plate-tectonic regime in the Archaean is mostly argued around geochemical evidence for the presence of arcs and/or spreading centres (Bédard et al., 2013). For example, most interpreted Archaean oceanic basalts have a crustal component (Pearce, 2008) and probably erupted on pre-existing continental crust; therefore, no Archaean oceanic lithosphere contains evidence for spreading (Kamber, 2015). On the other hand, many authors (Foley et al., 2002; Martin et al., 2005; Rollinson, 2010) argue that the Archaean TTG (tonalite–trondhjemite–granodiorite) suite, the dominant rock types in preserved Archaean crust (Hamilton, 2011), were generated in a convergent setting in island arcs above active subduction zones. Opponents argue that the Archaean TTG suites can be generated by vertical tectonics in plume-induced oceanic plateaus (Zegers and Keken, 2001; Bédard, 2006; Van Kranendonk, 2010; Kwelwa et al., 2017a) or from melting of ancient thick basaltic protocrust (Hamilton, 2011) with magmatism triggered by delamination of the lithospheric mantle. The distribution and rock record of sedimentary basins are a direct reflection of their tectonic setting (Dickinson and Valloni, 1980; Ingersoll and Busby, 1995). Of particular importance for deducing the tectonic setting of sedimentary basins is the detrital zircon record (Cawood et al., 2012). In this contribution we present detrital zircon age data and Hf isotopes which, in combination with the igneous, geochemical and zircon record can be used to infer the most likely tectonic and crustal growth scenario for the granite-greenstone terranes that outcrop south of Lake Victoria in the Archaean Tanzania Craton.

2. THE STRATIGRAPHY OF THE LATE ARCHAEOAN TANZANIA CRATON AND THE SIGNIFICANCE OF KAVIRONDIAN CONGLOMERATES

The stratigraphy of the Archaean Tanzania Craton (Fig. 1) is subdivided into the Dodoman, Nyanzian and the Kavirondian Supergroups (Manya et al., 2006; Kabete et al., 2012a; Sanislav et al., 2014). The Dodoman Supergroup, which is interpreted as basement and, thus, the oldest unit of the Tanzania Craton, mainly occurs in the central and southern part of the craton (Kabete et al., 2012a). No basement-age rocks have been identified so far in the northern half of the Tanzania Craton (Kabete et al., 2012b; Sanislav et al., 2014; Kwelwa et al., 2017b). The Sukumaland Greenstone Belt is dominated by the Nyanzian Supergroup and the associated granitoid intrusions (Fig. 1) with isolated occurrences of Kavirondian sediments. The stratigraphy is fragmented and disrupted by shear zones and granitoid intrusions (Borg and Shackleton, 1997; Sanislav et al., 2015). The Nyanzian Supergroup has been subdivided into Lower Nyanzian and Upper Nyanzian. The Lower Nyanzian (Fig. 3a) is dominated by deformed lower amphibolite facies mafic rocks of the Kiziba Formation (Cook et al., 2016) consisting of lava flows, pillow basalts, and dolerite and gabbro sills with minor shales and felsic volcanics. The Upper Nyanzian (Fig. 3a) consists of deformed, greenschist-facies, black shales and ironstones topped by a well bedded turbiditic sequence with volcanoclastic intercalations. The Kavirondian Supergroup (Fig. 3a) unconformably overlies the Nyanzian and comprises conglomerate, quartzite and grit. The Geita Greenstone Belt (Fig. 2) contains elements of the Nyanzian and the Kavirondian stratigraphy. In the Geita area the Kavirondian Supergroup consists mainly of quartzitic conglomerates that crop out in the northern part of the greenstone belt (Fig. 2) along a ~1km long and ~200m wide discontinuous zone trending more or less EW. The quartzitic conglomerates unconformably overlie the polydeformed Nyanzian ironstones. They have no consistent internal stratification, the clasts are generally well rounded (Fig. 3b), and in places a transition to coarse sandstone

can be observed. The conglomerates are poorly sorted and contain clasts of quartz-pebble conglomerate (Fig. 3b) suggesting some internal reworking and possibly re-sedimentation. The conglomerates contain a rich zircon population composed mostly of fragmented and sub-rounded grains which display concentric growth zoning (Fig. 3c) typical of igneous zircons.

3. ZIRCON AGE DISTRIBUTION AND GROWTH OF THE GRANITE-GREENSTONE TERRANE OF THE NORTHERN TANZANIA CRATON

The crustal growth of the Sukumaland Greenstone Belt as revealed by the zircon and rock record shows a progressive change in the igneous record from mafic to felsic igneous activity over a time span of ~200 Myr (Fig. 4a), between ~2820 Ma and ~2620 Ma (Kabete et al. 2012b; Sanislav et al., 2014; Kwelwa et al., 2017b). The earliest period of crustal growth, pre-2800 Ma, is dominated by widespread mafic-tholeiitic volcanism with isolated occurrences of felsic volcanics erupted in an oceanic plateau-like environment (Cook et al., 2016). Between 2780 Ma and 2700 Ma igneous activity was dominated by diorite and TTG assemblages synchronous with porphyries of similar composition. This was followed by a transition into a period dominated by felsic igneous rocks that culminated with widespread high-K granites intruding between 2660 Ma and 2620 Ma (Sanislav et al., 2014).

4. DETRITAL ZIRCON AGE RECORD AND LU–HF ISOTOPES OF THE KAVIRONDIAN CONGLOMERATES

Kavirondian conglomerates in the Geita Greenstone Belt contain zircons ranging in age from ~2790 Ma to ~2640 Ma (Fig. 4b), spanning almost the entire age spectrum obtained from igneous rocks in the northern half of the Tanzania Craton (Fig. 4a), with a major peak at

2715 Ma. Minor peaks can be recognised at 2750 Ma and 2690 Ma but the overall age population appears to reflect a normal distribution with a peak at 2715 Ma. The ϵ_{Hf} for the analysed zircon grains varies between +2.4 and -1.4 (Fig. 4c) with 98% of the positive ϵ_{Hf} values being present in zircon grains older than 2700 Ma. From 2700 Ma onwards only 41% of the zircon grains have positive ϵ_{Hf} (Fig. 4c). Overall, 86% of the ϵ_{Hf} data from the Kavirondian conglomerates show positive values suggesting a significant juvenile component in this part of the Tanzania Craton. Single stage depleted mantle model ages for all zircon grains vary from 2918 Ma to 3036 Ma which is similar to the ~3000 Ma model ages for the mafic volcanics of the Kiziba Formation (Manya, 2004; Manya and Maboko, 2008; Cook et al., 2016).

5. DETRITAL ZIRCON VS MAGMATIC AND GEOCHEMICAL RECORD

The two most striking aspects of the zircon age distribution seen in Figure 4 are the lack of any detrital zircon ages predating the extrusion of the mafic tholeiitic volcanics (Fig. 3a) and the fact that the igneous and the detrital ages cover a similar time period. The latter suggests that the detrital zircons were derived within the craton and record the crustal growth in this part of the Tanzania Craton. The detrital distribution also suggests that most zircons were derived from the TTG source, inasmuch as 70% of these zircons are older than 2700 Ma. The low representation of the high-K magmatism in the detrital population could indicate that the contribution of the high-K magmatism to the overall crustal volume is relatively small or poor exposure of equivalent rock types during sedimentation.

The lack of detrital zircon grains older than the mafic volcanics is consistent with earlier interpretations (Manya, 2004; Manya and Maboko, 2008; Cook et al., 2016) that the mafic volcanics of the Kiziba Formation are seen as the oldest rocks in this part of the

Tanzania Craton and were erupted through oceanic crust and represent true oceanic basalts. The origin of these mafic volcanics is important because their partial melting under eclogite- to amphibolite-facies conditions was considered to be the primary source of the TTGs (Maboko et al., 2006). Their geochemical and isotopic signature was interpreted to indicate partial melting in a back arc setting (Manya and Maboko, 2003; Manya and Maboko, 2008) or partial melting of a plume head in an oceanic plateau like setting (Cook et al., 2016). The main argument favouring a subduction component is the presence of a small negative Nb anomaly when normalized to NMORB, whereas primitive mantle ratios of the immobile and highly incompatible trace elements (Zr/Hf, Nb/Th, Ti/Zr, Nb/Y, Nb/U), bimodal volcanism and a short eruption time over a large area favours the plume head scenario. On Nb/Y–Zr/Y diagram, used to constrain the mantle source of oceanic basalts (Condie, 2003) most of the samples plot within the field of oceanic plateau basalts (Fig. 5a) consistent with a plume source although a few sample overlap with the fields of ocean ridge and arc basalts. The trend towards the arc basalts field can be interpreted to indicate subduction input, contamination with continental crust or the effect of alteration and metamorphism. Nb is considered immobile in most subduction systems whereas U and Th are considered mobile (e.g. Tatsumi, 1989; Plank and Langmuir, 1993; Elliot et al., 1997). Since all three elements are highly incompatible during melting and fractional crystallization, ratios such as Nb/Th and Nb/U can be used to track the mantle source composition of basalts, to trace the recycled continental crust, crustal contamination and alteration (e.g. Hofmann et al., 1986; Campbell, 2003; Hofmann, 2004; Pearce, 2008). In a subduction setting the addition of U and Th from the slab to the mantle wedge will lower the Nb/U and Nb/Th ratios of the melt. Contamination with crustal material or alteration and metamorphism will have a similar effect. The average Nb/U and Nb/Th ratios of the Kiziba Formation are 32 and 8 respectively (Fig. 5b), which are nearly identical to the primitive mantle values (Nb/U=34, Nb/Th=8; Sun

and McDonough, 1989). This corroborates Cook et al. (2016) interpretation that the Kiziba Formation basalts were extracted from a mantle source that did not experience previous crust extraction or subduction related modification. The Hf isotopic signature of the detrital zircons is dominated by positive ϵ_{Hf} values and follows an evolution curve with a $^{176}\text{Lu}/^{177}\text{Hf}$ ratio of 0.029, which is consistent with derivation from a mafic source. Moreover, the ϵ_{Hf} of the Kiziba Formation lies on the same evolution trend (Fig. 4c), which is consistent with interpretations (Maboko et al., 2006) that the mafic volcanics of the Kiziba Formation are the primary source for the TTGs. In fact, the high-K granites also plot along the same evolutionary trend (Fig. 4c) suggesting their derivation from the TTGs or from a mixed source of TTG and sediment with a TTG-like composition (Sanislav et al., 2014). This trend is also illustrated by the I-type character of both the TTGs and the high-K granites (Fig. 5c). The transition from TTG to high-K magmatism also marks a shift in the locus of melting (Fig. 5d), from the garnet stability field, characterised by high Sr/Y TTG granites, into the amphibolite field, characterised by low Sr/Y high-K granites.

6. A TECTONIC MODEL FOR CRUSTAL GROWTH

The petrological progression with time from mafic to felsic crust seen in the igneous record (Fig. 4a) is mirrored by the ϵ_{Hf} (Fig. 4c) of the detrital zircons and is consistent with a process in which juvenile mafic crust gradually matures into continental crust. This secular change appears to be characteristic for late Archaean, when the upper crust evolved from dominantly mafic, before 3 Ga, to dominantly felsic by 2.5 Ga (Dhuime et al., 2015; Yuan, 2015; Tang et al., 2016). From a geodynamic perspective this was interpreted to mark the transition from crust formed above mantle plumes to crust formed in subduction zones. Our observations from north-western Tanzania appear to conform to this global trend, therefore, a viable

geodynamic scenario has to explain the continuous evolution from mafic to felsic crust, the isotopic evolution, the distribution of the detrital zircons and the sedimentary record, and the composition of the mafic volcanics, the TTG and the high-K granites. The lack of any evidence of older crust involvement is inconsistent with a continental arc setting and the fact that modern island arcs are predominantly mafic in composition (e.g. Holbrook et al., 1999; Larter and Leat, 2003; Stern, 2010) precludes a direct comparison with modern island arc settings. The oceanic plateau-like composition (Fig. 5a) of the mafic volcanics and the fact that the isotopic and rock record is consistent with the generation of the TTGs by partial melting of mafic volcanics needs to be taken into account. Therefore, we propose a model in which crustal growth occurred by subduction modification of an oceanic plateau (Fig. 6a). The main period of TTG magmatism (Fig. 4) coincides with basin development and deposition of Nyanzian sediments (e.g. Borg and Krogh, 1999; Sanislav et al., 2014) followed by shortening between 2700 Ma and ~2660 Ma and finally late extension (van Ryt et al., 2017 synchronous with the emplacement of high-K granites (Sanislav et al., 2015; 2017). Therefore, most TTG magmatism occurred during an episode of extensional tectonics synchronous with the Upper Nyanzian sedimentation. Flat subduction was implied to explain the generation of TTGs in the Archaean (e.g. Smithies et al., 2003; Nutman et al., 2015; Hastie et al., 2016) but, at least in modern subduction systems, flat subduction is associated with compressional settings, wherein the arc migrates farther away from the trench and often the magmatic activity stops altogether (e.g. Gutscher et al., 2000; Sobolev and Babeico, 2005; Ducea et al., 2015). Slab steepening and subduction retreat may cause extension (Fig. 6b) in the overriding plate but slab dehydration will also cause melting in the mantle wedge (e.g. Ulmer, 2001; Stern, 2002; Stern, 2010). If that was the case, then most probably these mafic melts would have concentrated at the base of the oceanic plateau (Fig. 6b). Slab flattening at around 2700 Ma (Fig. 6c) caused basin inversion and initiated compression and a significant

drop in magmatism. By 2660 Ma enough thickening had occurred so that the base of the plateau delaminated and sank into the mantle (Fig. 6d). Upwelling of hot mantle heated up the crust to promote melting of TTG and related sediments with the formation of high-K granites, while partial melting of the metasomatised mantle was responsible for the emplacement of the lamprophyre dykes at around 2640 Ma (Borg, 1994; Borg and Krogh, 1999).

In conclusion, the tectonic model presented here takes into account the overall sedimentary, igneous and geochemical record and provides an explanation for the bell-shaped distribution of the detrital zircon population, which is consistent with internal reworking and progressive maturation of an oceanic plateau by successive partial melting events partly controlled by the changing nature of a subducting slab.

ACKNOWLEDGEMENTS

The authors thank Geita Gold Mine and AngloGold Ashanti for funding this work. Critical reviews by Peter Dahl and an anonymous reviewer are greatly acknowledged.

REFERENCES

- Bédard, J.H. (2006). A catalytic delamination-driven model for coupled genesis of Archaean crust and sub-continental lithospheric mantle. *Geochimica et Cosmochimica Acta*, 70, 1188–1214.
- Bédard, J.H., Harris, L.B., & Thurston, P.C. (2013). The hunting of the snArc. *Precambrian Research*, 229, 20–48.

- Borg, G. (1994). The Geita gold deposit in NW Tanzania – geology, ore petrology, geochemistry and timing of events. *Geologisches Jahrbuch*, 100, 545–595.
- Borg, G., & Krogh, T. (1999). Isotopic age data of single zircons from the Archaean Sukumaland greenstone belt, Tanzania. *Journal of African Earth Sciences*, 29, 301–312.
- Borg, G., & Shackleton R. M. (1997). The Tanzania and NE Zaire Cratons. In: de Wit, M.J., Ashwal, L.D. (Eds.) *Greenstone Belts*. Clarendon Press, Oxford, pp. 608-619.
- Campbell, I.H. (2003). Constraints on continental growth models from Nb/U ratios in the 3.5 Ga Barberton and other Archean basalt-komatiite suites. *American Journal of Science*, 303, 319–351.
- Cawood, P. A., Hawkesworth, C. J., & Dhuime, B. (2012). Detrital zircon record and tectonic setting. *Geology*, 40, 875– 78.
- Condie, K.C. (2003). Incompatible element ratios in oceanic basalts and komatiites: tracking deep mantle sources and continental growth rates with time. *Geochemistry, Geophysics, Geosystems*, 4 (1), 1-28.
- Cook, Y. A., Sanislav, I. V., Hammerli, J., Blenkinsop, T., & Dirks, P. H. G. M. (2016). A primitive mantle source for the Neoproterozoic mafic rocks from Tanzania Craton. *Geoscience Frontiers*, 7, 911-926.
- de Wit, M.J. (1998). On Archean granites, greenstones, cratons and tectonics: does the evidence demand a verdict? *Precambrian Research*, 91, 181–226.
- Dhuime, B., Wuestefels, A., Hawkesworth, C.J. (2015). Emergence of modern continental crust 3 billion years ago. *Nat. Geosci.* 8, 552–555.

- Dickinson, W. R. & Valloni, R. (1980). Plate settings and provenance of sands in modern ocean basins. *Geology*, 8, 82–86.
- Ducea, M.N., Saleeby, J.B., & Bergantz, G. (2015). The architecture, chemistry, and evolution of continental magmatic arcs. *Annual Review of Earth and Planetary Sciences*, 43, 299–331.
- Elliott, T., Plank, T., Zindler, A., White, W., & Bourdon, B. (1997). Element transport from slab to volcanic front at the Mariana Arc. *Journal of Geophysical Research*, 102, 14991–15019.
- Foley S., Tiepolo M., & Vannucci R. (2002). Growth of early continental crust controlled by melting of amphibolite in subduction zones. *Nature*, 417, 837–840.
- Gerya, T. (2014). Precambrian geodynamics: concepts and models. *Gondwana Research*, 25, 442-463.
- Gutscher, M.-A., Spakman, W., Bijwaard, H., & Engdahl, E.R. (2000). Geodynamics of flat subduction: seismicity and tomographic constraints from the Andean margin. *Tectonics*, 19, 814-833.
- Hamilton, W.B. (1998). Archean magmatism and deformation were not products of plate tectonics. *Precambrian Research*, 91, 143–179.
- Hamilton, W.B. (2011). Plate tectonics began in Neoproterozoic time, and plumes from deep mantle have never operated. *Lithos*, 123, 1–20.
- Hastie, A.R., Fitton, J.G., Bromiley, G.D., Butler, I.B., & Odling, N.W.A. (2016). The origin of Earth's first continents and the onset of plate tectonics. *Geology*, 44, 855–858.

- Hofmann, A. W. (2004). Sampling mantle heterogeneity through oceanic basalts: Isotopes and trace elements, in *Treatise on Geochemistry*, vol. 2, The Mantle and Core, edited by R. W. Carlson, pp. 61– 101, Elsevier, New York.
- Hofmann, A. W., Jochum, K. P., Seufert, H. M., & White, W. M. (1986). Nb and Pb in oceanic basalts: New constraints on mantle evolution. *Earth Planetary Science Letters*, 79, 33 –45.
- Holbrook, W. S., Lizarralde, D., McGeary, S., Bangs, N., & Diebold, J. (1999). Structure and composition of the Aleutian island arc and implications for continental crustal growth. *Geology*, 27, 31 – 34.
- Ingersoll, R.V. & Busby, C.J. (1995). Tectonics of sedimentary basins. In: Busby, C.J. & Ingersoll, R.V. (eds) *Tectonics of Sedimentary Basins*. Blackwell Science, Oxford, 1–51.
- Jelsma, H.A. & Dirks, P.H.G.M. (2002). Neoproterozoic tectonic evolution of the Zimbabwe Craton. In: C.M.R. Fowler, C. Ebinger and C.J. Hawkesworth (Editors), *The Early Earth: Physical, Chemical and Biological Development. Geological Society of London Special Publication*, 199, 183–211.
- Kabete, J.M., Groves, D.I., McNaughton, N.J., & Mruma, A.H. (2012a). A new tectonic and temporal framework for the Tanzanian Shield: implications for gold metallogeny and undiscovered endowment. *Ore Geology Reviews*, 48, 88-124.
- Kabete, J.M., McNaughton, N.J., Groves, D.I., & Mruma, A.H. (2012b). Reconnaissance SHRIMP U–Pb zircon geochronology of the Tanzania Craton: Evidence for Neoproterozoic granitoid–greenstone belts in the Central Tanzania Region and the Southern East African Orogen. *Precambrian Research*, 216– 219, 232– 266.

- Kamber, B.S. (2015). The evolving nature of terrestrial crust from the Hadean, through the Archaean, into the Proterozoic. *Precambrian Research*, 258, 48–82.
- Kwelwa, S. D., Sanislav, I. V., Dirks, P. H. G. M., Blenkinsop, T. Kolling, S. L. (2017a). The petrogenesis of the Neoproterozoic Kukuluma Intrusive Complex, NW Tanzania. *Precambrian research* – in press.
- Kwelwa, S.D., Sanislav, I.V., Dirks, P.H.G.M., Blenkinsop, T., Kolling, S.L. (2017b). Zircon U-Pb ages and Hf isotope data from the Kukuluma Terrain of the Geita Greenstone Belt, Tanzania Craton: implications for stratigraphy, crustal growth and timing of gold mineralization. *Journal of African Earth Sciences* – in press.
- Larter, R.D., & Leat, P.T. (2003). Intra-Oceanic Subduction Systems: Tectonic and Magmatic Processes. *Geological Society of London Special Publication*, 219, 1-17.
- Maboko, M.A.H., Pedersen, R.B., Many, S., Torssander, P., & Mwache, M. (2006). The origin of late Archaean granitoids in the Sukumaland greenstone belt of northern Tanzania: geochemical and isotopic constraints. *Tanzania Journal of Science*, 32, 75–86.
- Many, S. (2004). Geochemistry and petrogenesis of volcanic rocks of the Neoproterozoic Sukumaland greenstone belt, northwestern Tanzania. *Journal of African Earth Sciences*, 40, 269–279.
- Many, S., & Maboko, M.A.H. (2003). Dating basaltic volcanism in the Neoproterozoic Sukumaland Greenstone Belt of the Tanzania Craton using the SmNd method: implications for the geological evolution of the Tanzania Craton. *Precambrian Research*, 121, 35-45.

- Manya, S., & Maboko, A. H. M. (2008). Geochemistry of the Neoproterozoic mafic volcanic rocks of the Geita area, NW Tanzania: Implications for stratigraphical relationships in the Sukumaland greenstone belt. *Journal of African Earth Sciences*, 52, 152-160.
- Manya, S., Kobayashi, K., Maboko, M.A.H., & Nakamura, E. (2006). Ion microprobe zircon U-Pb dating of the late Archean metavolcanics and associated granites of the Musoma-Mara Greenstone Belt, Northeast Tanzania: Implications for the geological evolution of the Tanzanian Craton. *Journal of African Earth Sciences*, 45, 355-366.
- Martin, H., Smithies, R.H., Rapp, R., Moyen, J.F., & Champion, D. (2005). An overview of adakite, tonalite–trondhjemite–granodiorite (TTG), and sanukitoid: relationships and some implications for crustal evolution. *Lithos*, 79, 1–24.
- Mints, M.V., Belousova, E.A., Konilov, A.N., Natapov, L.M., Shchipansky, A.A., Griffin, W.L., O'Reilly, S.Y., Dokukina, K.A., & Kaulina, T.V. (2010). Mesoproterozoic subduction processes: 2.87 Ga eclogites from the Kola Peninsula, Russia. *Geology*, 38, 739–742.
- Moyen, J.F., & van Hunen, J. (2012). Short-term episodicity of Archean plate tectonics. *Geology*, 40, 451-454.
- Nutman, A.P., Bennett, V.C., & Friend, C.R.L. (2015). The emergence of the Eoarchean proto-arc: Evolution of a c. 3700 Ma convergent plate boundary at Isua, southern West Greenland, in Roberts, N.M.W., et al., eds., *Continent Formation through Time. Geological Society of London Special Publication*, 389, 113–133.
- Pearce, J. A. (2008). Geochemical fingerprinting of oceanic basalts with applications to ophiolite classification and the search for Archean oceanic crust. *Lithos*, 100, 14–48.
- Plank, T., & Langmuir, C. H. (1993). Tracing trace elements from sediment input to volcanic output at subduction zones. *Nature*, 362, 739 – 742.

- Accepted Article
- Rey, P. F., Coltice, N., & Flament, N. (2015). Spreading continents kick-started plate tectonics. *Nature*, 513, 405–408.
- Rollinson, H. (2010). Coupled evolution of Archean continental crust and subcontinental lithospheric mantle. *Geology*, 38, 1083–1086.
- Sanislav, I. V., Brayshaw, M., Kolling, S. L., Dirks, P. H. G. M., Cook, Y. A., & Blenkinsop, T. (2017). The structural history and mineralization controls on the world-class Geita Hill gold deposit, Geita Greenstone Belt, Tanzania. *Mineralium Deposita*, 52, 257-279.
- Sanislav, I. V., Wormald, R. J., Dirks, P. H. G. M., Blenkinsop, T. G., Salamba, L., & Joseph, D. (2014). Zircon U-Pb ages and Lu-Hf isotope systematics from late-tectonic granites, Geita greenstone belt: implications for crustal growth of the Tanzania craton. *Precambrian research*, 242, 187-204.
- Sanislav, I.V., Kolling, S.L., Brayshaw, M., Cook, Y.A., Dirks, P.H.G.M., Blenkinsop, T.G., Mturi, M.I., & Ruhega, R. (2015). The geology of the giant Nyankanga gold deposit, Geita Greenstone Belt, Tanzania. *Ore Geology Reviews*, 69, 1-16.
- Smithies, R.H., Champion, D.C., & Cassidy, K.F. (2003). Formation of Earth's early Archaean continental crust. *Precambrian Research*, 127, 89–101
- Sobolev, S.V., & Babeyko, A.Y. (2005). What drives orogeny in the Andes? *Geology*, 33, 617–620.
- Stern, R. J. (2002). Subduction zones. *Reviews of Geophysics*, 40.
- Stern, R.J. (2005). Evidence from ophiolites, blueschists, and ultrahigh-pressure metamorphic terranes that the modern episode of subduction tectonics began in Neoproterozoic time. *Geology*, 33, 557–560.

- Stern, R.J. (2010). The anatomy and ontogeny of modern intra-oceanic arc systems. *Geological Society Special Publication*, 338, 7–34.
- Sun, S.-S., McDonough, W.F. (1989). Chemical and isotopic systematics of oceanic basalts: implications for mantle composition and processes. In: Saunders, A.D., Norry, M.J. (Eds.), *Magmatism in the Ocean Basins. Geological Society, London, Special Publications*, 313-345.
- Tang, M., Chen, K., Rudnick, R.L. (2016). Archean upper crust transition from mafic to felsic marks the onset of plate tectonics. *Science* 351, 372–375.
- Tatsumi, Y. (1989). Migration of fluid phases and genesis of basalt magmas in subduction zones. *Journal of Geophysical Research*, 94, 4697– 4707.
- Ulmer, P. (2001). Partial melting in the mantle wedge—The role of H₂O in the genesis of mantle-derived ‘arc-related’ magmas. *Physics of the Earth and Planetary Interiors*, 127, 215–232.
- van Hunen, J., & Moyen, J.-F. (2012). Archaean subduction: fact or fiction? *Annual Review of Earth and Planetary Sciences*, 40, 195–219.
- Van Kranendonk, M.J. (2010). Two types of Archean continental crust: plume and plate tectonics on early Earth. *American Journal of Science*, 310, 1187-1209.
- Van Kranendonk, M.J., Collins, W.J., Hickman, A., & Pawley, M.J. (2004). Critical tests of vertical vs. horizontal tectonic models for the Archaean East Pilbara Granite-Greenstone Terrane, Pilbara Craton, Western Australia. *Precambrian Research*, 131, 173–211.
- Van Kranendonk, M.J., Smithies, R.H., Hickman, A.H., & Champion, D.C. (2007). Secular tectonic evolution of Archean continental crust: interplay between horizontal and vertical processes in the formation of the Pilbara Craton, Australia. *Terra Nova*, 19, 1-38.
- van Ryt, M., Sanislav, I. V., Dirks, P.H.G.M. Huizenga, J.M., Mturi, M. I., Kolling, S.L. (2017). Alteration paragenesis and the timing of mineralised quartz veins at the world-

class Geita Hill gold deposit, Geita Greenstone Belt, Tanzania. *Ore Geology Reviews* – in press.

Vervoort, J.D., & Blichert-Toft, J. (1999). Evolution of the depleted mantle: Hf isotope evidence from juvenile rocks through time. *Geochimica et Cosmochimica Acta*, 63, 533-556.

Wang, J., Kusky, T., Polat, A., Wang, L., Deng, H., & Wang, S. (2013). A late Archean tectonic mélangé in the Central Orogenic Belt, North China Craton. *Tectonophysics*, 608, 929–946.

Yuan, H. (2015). Secular change in Archaean crust formation recorded in Western Australia. *Nat. Geosci.* 8, 808–813.

Zegers, T.E., & van Keken, P.E. (2001). Middle Archean continent formation by crustal delamination. *Geology*, 29, 1083–1086.

Supplementary material:

Analytical procedures and protocols

Table S1. Table with the analytical results and the calculated ages for the Kavirondian conglomerates.

Table S2. Table with the analytical results and the calculated ages for the GJ1 standard.

Table S3. Table with the analytical results and the calculated ages for the Temora standard.

Table S4. Table with the analytical results and the calculated ages for the 91500 standard.

Table A1. Lu-Hf isotope data and time corrected parameters of zircons from the Kavirondian conglomerates.

Figure captions

Figure 1

Simplified geological map of northern Tanzania showing the main tectonic and geological units (modified from Sanislav et al., 2015). SU – Sukumaland Greenstone Belt; NZ – Nzega Greenstone Belt; SM – Shynianga-Malita Greenstone Belt; IS – Iramba-Sekenke Greenstone Belt; KF – Kilimafedha Greenstone Belt; MM – Musoma-Mara Greenstone Belt. Inset shows the location of Tanzania Craton on the African continent.

Figure 2

Geological map of Geita Greenstone Belt showing the main lithological units and the location of the Kavirondian conglomerates.

Figure 3

(a) Simplified stratigraphic column of the Nyanzian and Kavirondian Supergroups. (b) Field photograph of the quartzitic Kavirondian conglomerates that outcrop in Geita Greenstone Belt. Note the rounded to subrounded, poorly sorted quartzitic clasts and the presence of conglomerate fragments. (c) CL images showing the ages (Ma) and locations of analytical spots for selected zircon grains separated from the Kavirondian conglomerates. Note the fragmented and subrounded nature of the zircon grains.

Figure 4

Distribution of igneous zircon ages (a) from the northern half of the Tanzania Craton and the dominant rock types (dataset from Sanislav et al., 2014). (b) Distribution of detrital zircon ages separated from the Kavirondian conglomerates. Note the almost perfectly symmetrical bell-shaped curve. (c) Plot of ϵ_{Hf} versus age for the detrital zircons separated from the Kavirondian conglomerates. The ϵ_{Hf} for the Kiziba Formation was calculated based on Vervoort and Blichert-Toft (1999) from the ϵ_{Nd} values (Manya and Maboko, 2008; Cook et al., 2016). The ϵ_{Hf} data for the high-K granites (Sanislav et al., 2014) plot near the chondritic

evolution line. All data can be explained by an evolution line corresponding to a $^{176}\text{Lu}/^{177}\text{Hf}$ ratio of 0.029 typical of mafic rocks.

Figure 5

Series of plots showing some key geochemical characteristics of the mafic volcanics (a and b), the TTG and the high-K granites (c and d). On Zr/Y–Nb/Y diagram (a; modified from Cook et al., 2016) the mafic volcanics plot near the primitive mantle composition in the oceanic plateau basalts field corresponding to plume related sources (data from Many, 2004; Many and Maboko, 2008; Cook et al., 2016). On Nb/Th–Nb/U diagram (b) the mafic volcanics plot near the primitive mantle composition away from the normal mid-ocean ridge (NMORB) and island arc basalts (IAB). Primitive mantle incompatible trace elements ratio suggests that the mantle source of the Kiziba Formation mafics did not experience previous crust extraction or subduction modification. The Na_2O vs K_2O diagram (c) shows that most of the TTG and high-K granites have I-type characteristics ($\text{Na}_2\text{O} > 3.2\%$; $\text{A/CNK}=0.9\text{--}1.1$; amphibole bearing). The petrogenesis of the high-K granites (2660–2620 Ma) involved melting of TTG and TTG derived immature sediments (Sanislav et al., 2014). The Sr/Y vs Y diagram (d) shows that the TTG petrogenesis (<2700 Ma) involved melting in the garnet stability field with melts generated at the base of the crust (Maboko et al., 2006) whereas the petrogenesis of the high-K granites (2660–2620 Ma) occurred at higher crustal levels. EMORB-enriched mid-ocean ridge basalt; OIB – ocean island basalt; UCC – upper continental crust.

Figure 6

Series of cartoons illustrating a possible tectonic model for the crustal growth of the northern Tanzania Craton. The diagram on the right-hand side of each cartoon shows the detrital zircon distribution and the ϵ_{Hf} evolution line corresponding to different stages of crustal growth. a) Pre-2800 Ma eruption of mafic volcanics of the Kiziba Formation in an oceanic-

Accepted Article

plateau-like environment with the development of a thick oceanic root. b) >2700 Ma a subduction zone initiates and slab roll-back causes extension in the overriding oceanic plateau and deposition of the Upper Nyanzian sediments. Due to the thickness of the plateau, melts generated by slab dehydration cannot ascend and accumulate at the base of the plateau (now mostly eclogite), which starts to melt generating diorite and TTG. c) A switch to flat-slab subduction causes compression in the overriding oceanic plateau and a dramatic reduction in magma production. d) The eclogitised slab delaminates and sinks into the mantle, and the ascent of hot mantle at the base of the plateau causes heating and partial melting of TTG and Nyanzian sediments to generate high-K granites. Some metasomatised mantle melts penetrate into the plateau in the form of lamprophyre dykes.

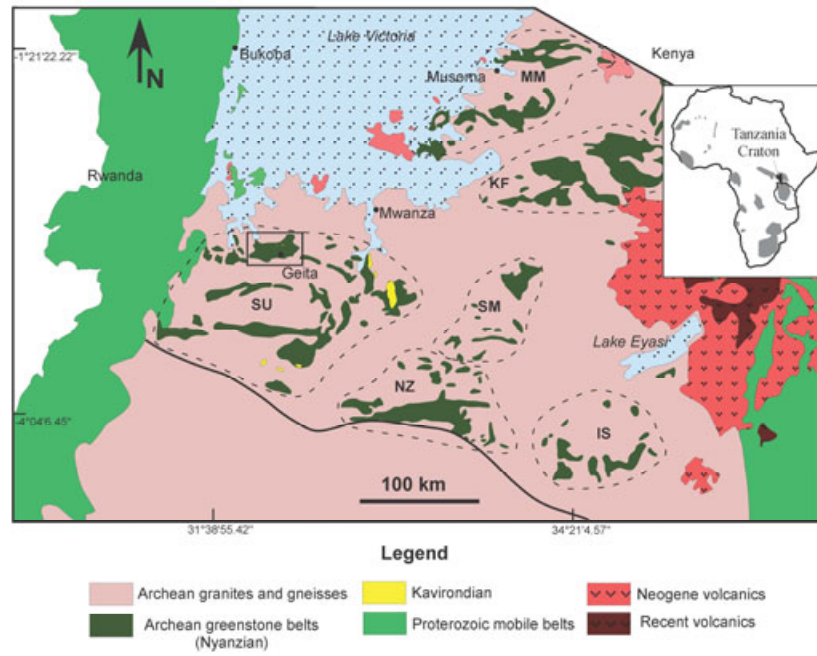


Figure 1

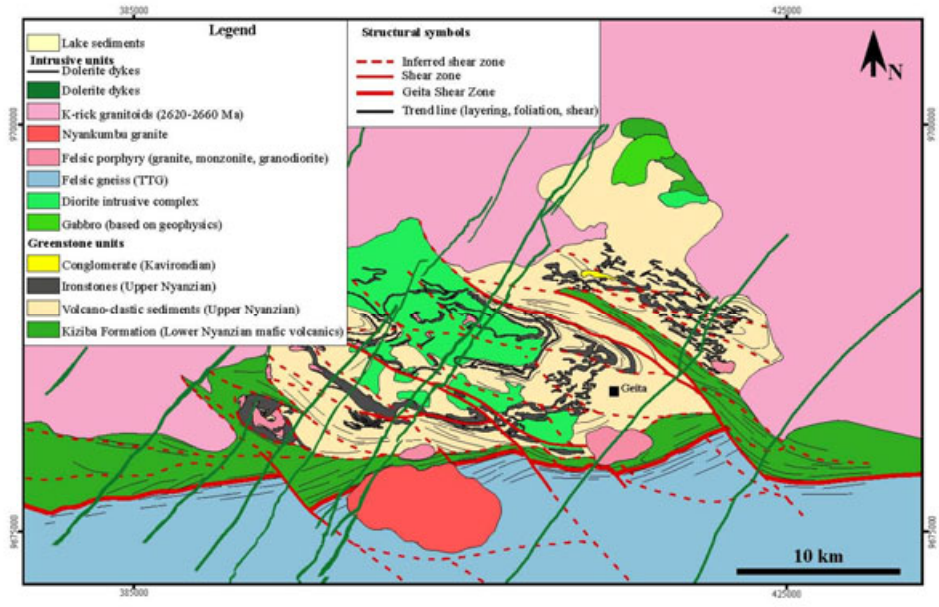


Figure 2

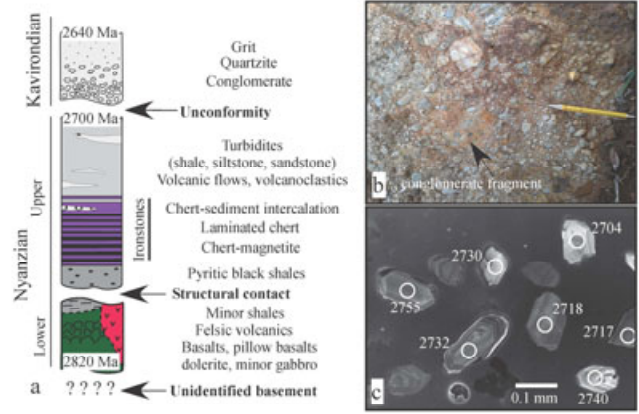


Figure 3

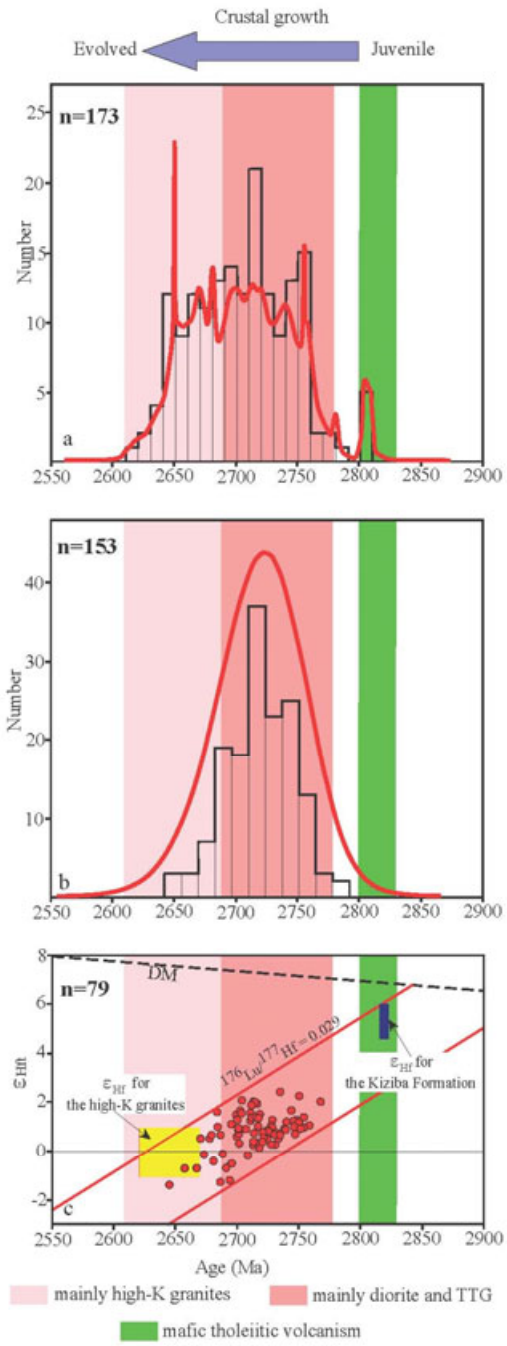


Figure 4

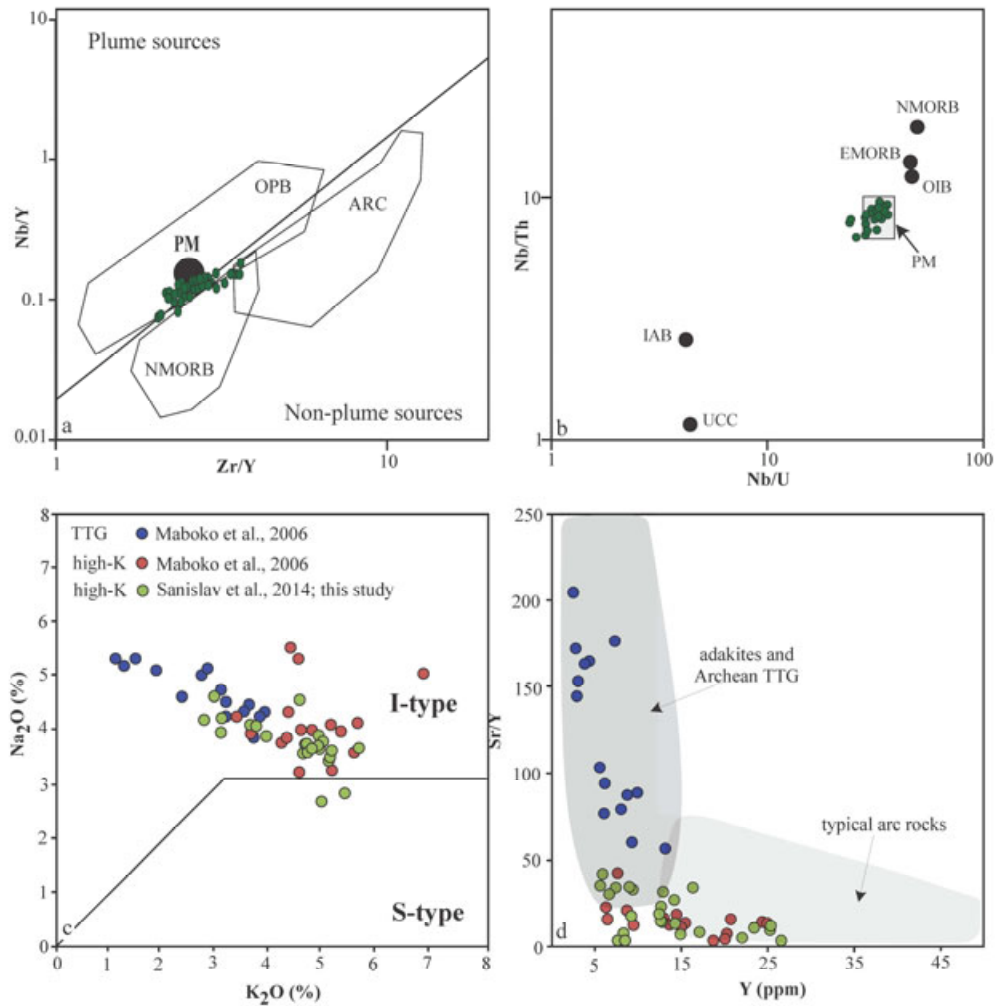


Figure 5

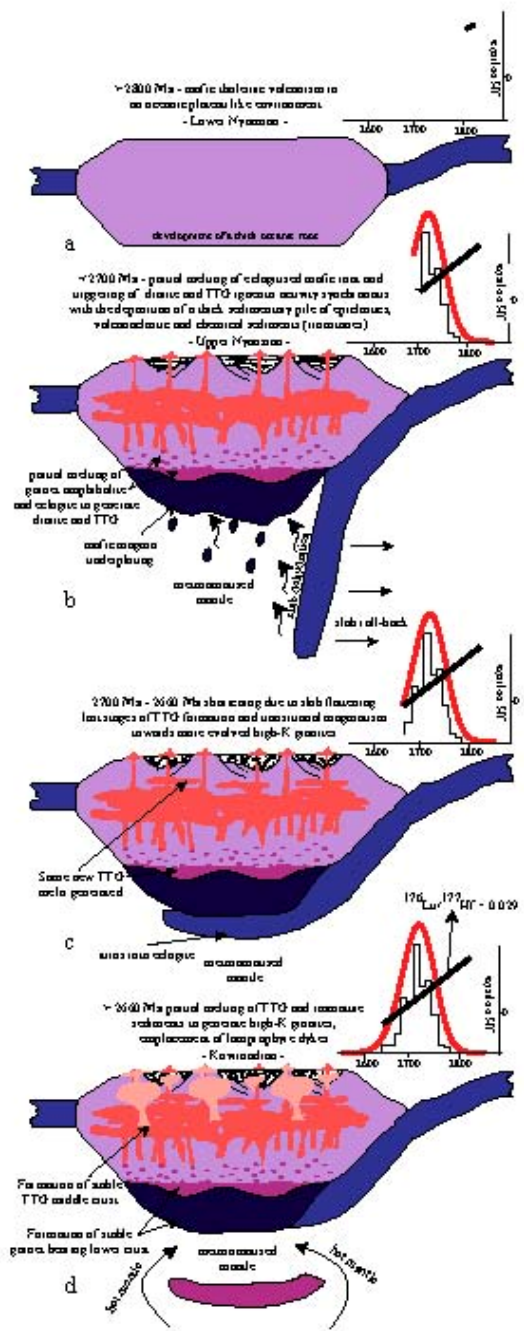


Figure 6